

Article

Self-Assembled Three-Dimensional Microporous rGO/PNT/Fe₃O₄ Hydrogel Sorbent for Magnetic Preconcentration of Multi-Residue Insecticides

Sheng Wang, Xiuqin Li, Ming Li, Xianjiang Li , Xiaomin Li, Shuangqing Li, Qinghe Zhang and Hongmei Li *

Division of Chemical Metrology and Analytical Science, National Institute of Metrology, Beijing 100029, China; wangsh@nim.ac.cn (S.W.); lixq@nim.ac.cn (X.L.); liming@nim.ac.cn (M.L.); lixianjiang@nim.ac.cn (X.L.); lixm@nim.ac.cn (X.L.); lishuangqing17@mails.ucas.ac.cn (S.L.); zhangqh@nim.ac.cn (Q.Z.)

* Correspondence: lihm@nim.ac.cn; Tel.: +86-10-64524701

Received: 24 June 2020; Accepted: 2 August 2020; Published: 15 August 2020



Abstract: The purpose of this work was to develop a highly selective, sensitive, and reliable method for multi-residual analysis. A three-dimensional microporous reduced graphene oxide/polypyrrole nanotube/magnetite hydrogel (3D-rGOPFH) composite was synthesized and utilized as a magnetic solid-phase extraction (MSPE) sorbent to preconcentrate thirteen insecticides, including five organophosphorus (isocarbophos, quinalphos, phorate, chlorpyrifos, and phosalone), two carbamates (pirimor and carbaryl), two triazoles (myclobutanil and diniconazole), two pyrethroids (lambda-cyhalothrin and bifenthrin), and two organochlorines (2, 4'-DDT and mirex), from vegetables, followed by gas chromatography-tandem mass spectrometry. This method exhibited several major advantages, including simultaneous enrichment of different types of insecticides, no matrix effect, high sensitivity, and ease of operation. This is ascribed to the beneficial effects of 3D-rGOPFH, including the large specific surface (237 m² g⁻¹), multiple adsorption interactions (hydrogen bonding, electrostatic, π - π stacking and hydrophobic interaction force), appropriate pore size distribution (1–10 nm), and the good paramagnetic property. Under the optimal conditions, the analytical figures of merit were obtained as: linear dynamic range of 0.1–100 ng g⁻¹ with determination coefficients of 0.9975–0.9998; limit of detections of 0.006–0.03 ng g⁻¹; and the intra-day and inter-day relative standard deviations were 2.8–7.1% and 3.5–8.8%, respectively. Recoveries were within the range of 79.2 to 109.4% for tomato, cucumber, and pakchoi samples at the fortification levels of 5, 25, and 50 ng g⁻¹. This effective and robust method can be applied for determining multi-classes of insecticide residues in vegetables.

Keywords: insecticides; vegetables; gas chromatography-tandem mass spectrometry; magnetic solid-phase extraction; three-dimensional microporous composite

1. Introduction

Insecticides (e.g., organophosphorus pesticides (OPPs), organochlorine pesticides (OCPs), pyrethroids, and carbamates) are widely used for pest control in agriculture and residential places. Nevertheless, many insecticides are carcinogenic, teratogenic, and mutagenic to human cells. Long-term accumulation in vivo of insecticides can seriously harm the nervous, genital, and immune systems of the human body [1]. Maximum residue limits (MRLs) were set strictly by many organizations toward insecticides. For instance, the European Union (EU) has set the MRLs at 0.01–0.3 $\mu\text{g g}^{-1}$ for insecticides, such as OPPs and pyrethroids, in vegetables [2]. Therefore, developing an effective analytical method for trace-level determination of insecticide residues is indispensable and highly necessary.

Extensive research has been performed to develop the analytical methods and techniques for insecticide residues [3,4], especially for the simultaneous determination of multiresidues. Owing to its high separation ability and satisfactory qualitative and quantitative performance, chromatographic technology is often employed to measure insecticides in different samples. Gas chromatography (GC) and liquid chromatography (LC) equipped with mass spectrometers, such as single quadrupole or triple quadrupole, are frequently utilized for the accurate and rapid qualification and quantification of insecticide residues in food samples. Despite the advantages, multiresidue analysis suffers from the interference from matrix compounds, which compromises accuracy, replicability, and sensitivity of the analysis. Therefore, the separation of pesticides from complex food samples before chromatographic analysis is usually a critical procedure. Many sample preparation techniques have been applied to extract and preconcentrate the pesticides, such as liquid–liquid extraction [5], solid-phase extraction (SPE) [6], solid-phase microextraction (SPME) [7], dispersive liquid–liquid microextraction (DLLME) [8], and dispersion-solidification liquid–liquid microextraction [9].

Magnetic solid-phase extraction (MSPE), integrating extraction and separation, as well as clean-up and concentration of analytes into a single step, has attracted much attention in sample pretreatment. For MSPE, magnetic sorbents are directly dispersed into sample solutions, and the dispersive mode facilitates the increase of interfacial area between analytes and sorbents. Therefore, the extraction efficiency of MSPE can be improved compared with the conventional SPE. Moreover, the use of magnetic sorbent makes the phase separation step much convenient and avoids the traditional centrifugation or filtration process. Among different materials, graphene-based magnetic nanomaterials have received great attention owing to their unique physicochemical properties [10,11], high surface-to-volume ratio, and large sorption capacity. A few research groups have managed to fabricate magnetic graphene nanomaterials for the preconcentration or removal of some pollutant residues [12,13]. However, recent studies have shown that restacking and agglomeration of graphene sheets are difficult to avoid while synthesizing magnetic composites [14]; restacking and agglomeration may decrease the specific surface area of graphene, affecting its extraction efficiency. The restricted selectivity of graphene is another limitation. Generally, graphene material is a non-polar, hydrophobic sorbent with sp^2 -hybridized carbon atoms, and they show a partial affinity for hydrophobic compounds/aromatic structure and interact weakly with polar, ionic or other types of compounds [15]. The extraction efficiency of graphene material is easily limited for some types of target analytes, which was undesired for analysis of multi-class residues [16]. Additionally, many undesired impurities would be extracted from the sample matrix along with the analyte, affecting the analytical performance of the methods [17]. Therefore, some selective sorbents and methods should be developed for ensuring high analyte recoveries, good sensitivity, and low levels of co-extracted matrix compounds.

Three-dimensional (3D) nanomaterials, with ultrahigh specific area, micropores, faster mass and electronic transport kinetics, and functional properties, provide great potentials for solving the above-mentioned problems. The 3D architectures with controlled micro- and nanostructure have been mainly used in supercapacitors, gas storage, sensors, batteries, and catalysis [18]. Hitherto, the studies on fabricating of 3D graphene-based composites and their application as sorbents have rarely been reported [19]. Within the past few years, much effort has been paid to the development of strategies for fabricating 3D-G architectures and compositions of graphene with other materials, e.g., carbon nanotubes, polymers, and metal oxides [20,21]. A simple method for fabrication of a 3D microporous reduced graphene oxide (rGO)/polypyrrole nanotube (PNT)/magnetite (Fe_3O_4) hydrogel (3D-rGOPFH) nanohybrid is the self-assembly of graphene oxide (GO), PNT, and Fe_3O_4 nanoparticles in a one-step hydrothermal reduction [22]. PNT was employed as a spacer between graphene sheets to avoid the stacking or aggregation of graphene sheets during the chemical reduction process, and a 3D porous structure of hydrogel with the high specific area was obtained. Polypyrrole is an advanced material of conducting polymer that is cheap, stable, and has good mechanical strength. Polypyrrole contains abundant–NH functional groups, large π -conjugated, and linear carbon chain structure, which is promising in separation science owing to its versatile properties such as hydrogen bonding, ion

exchange property, electroactivity, hydrophobicity, large π -conjugated structure, and so on [23]. On the basis of these versatile properties, PNT is expected to improve the adsorption ability of graphene for different classes of insecticides. Additionally, a previous study showed that appropriate pores of nanomaterials could exclude large compounds but allow small compounds to enter, resulting in the separation of compounds with different molecular sizes [24]. The interference compounds in the extract of vegetable matrices are usually long alkyl chains-containing phenols, esters, acids, and alcohols [25]. These large molecules are usually in oligomers larger than 10 nm [26], while the molecular size of a pesticide is relatively small (sub-nanometer level) [27,28]. So, the pesticides can be separated from the vegetable matrices by porous material with a proper pore size, which will minimize the reduction of the matrix effects. The 3D-rGOPFH combines the virtue of 3D architecture of rGO, PNT, and Fe_3O_4 nanoparticles, which makes it a promising sorbent for different compounds in sample preparation techniques.

In this study, the 3D-rGOPFH nanocomposite was synthesized according to the recently reported method [22] and its potential application for the enrichment of insecticide residues in vegetables was studied. Thirteen insecticides, including widely applied OPPs, OCPs, pyrethroids, triazoles, and carbamates, were selected as representative targets, and gas chromatography-tandem mass spectrometry (GC-MS/MS) was performed for the study. The results demonstrated that this is a simple, sensitive, and effective MSPE method for the detection of multi-insecticide residues in vegetables.

2. Materials and Methods

2.1. Chemicals and Reagents

Pyrrole monomer ($\geq 98\%$) was purchased from Sigma–Aldrich (Shanghai, China). Sodium 4-[4'-(dimethylamino)-phenyldiazo] phenylsulfonate ($\geq 99.9\%$), iron (III) chloride (FeCl_3 , $\geq 99.9\%$), iron (II) chloride tetrahydrate ($\text{FeCl}_2 \cdot 4\text{H}_2\text{O}$, $\geq 99.9\%$), phytic acid (50% in water), and ammonium peroxydisulfate ($\geq 99\%$) were bought from J&K Chemical (Beijing, China). All solvents were of HPLC grade and purchased from Merck (Darmstadt, Germany). GO powder was procured from Xianfeng Nanomaterials Technology Co., Ltd. (Nanjing, China). Ultrapure water ($18.2 \text{ M}\Omega/\text{cm}$) was prepared by a Synergy System from Thermo (Pittsburgh, PA, USA).

Different analytical standards of insecticides, including isocarbophos (GBW(E)060544, 99.5%), quinalphos (GBW(E)060995, 99.8%), pirimor (GBW(E)060890, 99.5%), carbaryl (GBW(E)060223, 99.9%), myclobutanil (GBW(E)060979, 99.9%), diniconazole (GBW(E)060885, 99.5%), lambda-cyhalothrin (GBW(E)061099, 99.5%), and bifenthrin (GBW(E)060548, 99.6%), were received from the National Institute of Metrology (NIM, Beijing, China). Phorate (99.3%), chlorpyrifos (99.4%), phosalone (99.0%), 2,4'-DDT (99.2%), and mirex (99.0%) were purchased from AccuStandard Inc. (New Heaven, CT, USA). A mixed stock standard solution was prepared at a concentration of $10 \mu\text{g g}^{-1}$ in acetone. A series of working standard solutions at different concentrations were prepared by appropriately diluting of the stock standard solution with acetone to achieve the desired concentration. All the standard solutions were stored at -20°C in the dark until use.

2.2. Synthesis of the Sorbent Materials

Fe_3O_4 nanoparticles were synthesized according to the chemical co-precipitation method. 6 g of $\text{FeCl}_2 \cdot 4\text{H}_2\text{O}$ and 10 g of FeCl_3 were dispersed in 50 mL of water with 2 mL of HCl, and then the mixture was added dropwise into 250 mL of 1.5 M NaOH aqueous solution under vigorous stirring. A black precipitate was obtained by centrifugation at $3000 \times g$ (20°C , 2 min), and the precipitate was washed with water for three times. Then 250 mL of a 0.01 M HCl solution was added to neutralize the anionic charges on the nanoparticles. Synthetic product was collected and dried at 50°C under vacuum.

PNT was fabricated according to a static assembly and freeze-drying method [29]. Briefly, 26.4 mg of ammonium peroxydisulfate was dissolved in 200 mL of sodium 4-[4'-(dimethylamino)-phenyldiazo] phenylsulfonate aqueous solution (5 mmol). Then, 1 mL of pyrrole monomer and 0.2 mL of phytic

acid was added dropwise into the mixture under vigorous stirring for 2 min at room temperature, the mixture was then allowed to stand without stirring for 12 h at 4 °C to achieve a black hydrogel. The PNT was washed with water/ethyl alcohol ($v/v = 1:1$) and then freeze-dried overnight.

The 3D-rGOPFH was synthesized through a hydrothermal reduction method [22,30]. First, 18.5 mg of GO powder was dispersed in 20 mL of ultrapure water by ultrasonic treatment (40 kHz) for 5 min. Then, 221.5 mg of PNT and 240 mg of Fe_3O_4 nanoparticles were added, and the dispersion was continuously stirred for 8 h at room temperature. Then, 380 μL of hydrazine hydrate (80%) was added dropwise into it. The as-prepared solution was sealed and heated at 90 °C for 12 h. A self-assembly process then occurred. The scheme shown in Figure 1 is similar to fishing with a fishing net. The fish were the PNT and Fe_3O_4 nanoparticle, and the fishing net was GO nanosheets. All of them self-assembled together to form a 3D network architecture during the reduction process. After cooling, the resulting intumescent hydrogel was rinsed with water/ethyl alcohol ($v/v = 1:1$) three times to remove impurities. Finally, the target product was collected with an external magnet and freeze-dried.

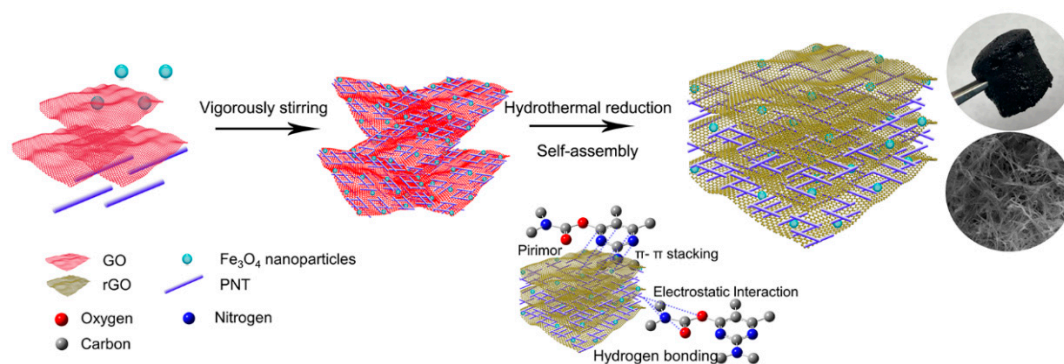


Figure 1. The schematic illustration of the synthetic process of the 3D-rGOPFH.

The synthesis of PNT/ Fe_3O_4 refers to the above-mentioned method, the conditions of synthesis were the same except for the addition of GO powder. 3D graphene nanocomposite (3D-G- Fe_3O_4) was synthesized by a vacuum free-dried method [31]. The 2D graphene nanocomposite (2D-G- Fe_3O_4) was synthesized following the method of Wang et al. [32].

2.3. Instrument

The GC-MS/MS experiments were performed using the Thermo Scientific TSQ 8000 EVO triple quadrupole mass spectrometer coupled with a Trace 1310 gas chromatograph and a TriPlus RSH autosampler (Thermo Fisher Scientific, Austin, TX, USA). An Agilent J&W Scientific DB-5MS (30 m \times 0.25 mm, 0.25 μm) capillary column was used for GC separation. The temperatures of the injector, transfer line, and ion source were maintained at 250 °C, 280 °C and 280 °C, respectively. The column oven temperature was programmed with an initial temperature of 60 °C for 1 min, raised to 230 °C with a rate of 20 °C min^{-1} (hold for 5 min), and finally ascended to 290 °C at 30 °C min^{-1} (hold for 6 min). Ultra-high-purity helium (99.999%) was used as the carrier gas at a constant flow rate of 1.0 mL min^{-1} . All the samples were analyzed in electron ionization (EI) and multiple reaction monitoring modes (MRM). The detailed information of the characteristic ions and the retention time of all insecticides are listed in Table S1.

The morphology and size of the sorbent materials were characterized using scanning electron microscopy (SEM, JSM-6330FT, JEOL, Tokyo, Japan) and transmission electron microscopy (TEM, JEM-2010, JEOL, Tokyo, Japan). Infrared absorption spectra were obtained using a NICOLET AVATAR 330 Fourier-transform infrared (FT-IR, Thermo Fisher Scientific, Waltham, MA, USA) spectrometer. X-ray diffractometry (XRD) experiments were carried out using a Shimadzu XRD-6000 (Shimadzu, Kyoto, Japan) with Cu $K\alpha$ radiation (40 kV, 30 mA, $\lambda = 1.5418 \text{ \AA}$), recorded with 2θ ranging from

5° to 90°. The nitrogen adsorption/desorption measurements were conducted by a Quantachrome AUTOSORB-SI instrument. The magnetic property was examined using a SQUID-based magnetometer (Quantum Design, San Diego, CA, USA).

2.4. Sample Preparation

The fresh vegetable samples were obtained from different local supermarkets and were previously checked to be free from the target insecticides. The analytical portion of samples was chopped and homogenized with a blender for 2 min at room temperature and stored at −20 °C until analysis. The homogenized sample (10 ± 0.01 g) was weighed into a 50 mL of polytetrafluoroethylene centrifuge tube. A known amount of the fortification standard solution (refer to recovery studies) was added and the sample was left for 30 min before the extraction. Ten milliliters of the water-methanol mixture (1:10, *v/v*) was added into it. The mixture was vigorously shaken for 1 min and centrifugated at 3000× *g* (20 °C) for 5 min. Then, the resulting supernatant was filtered through a 0.45 μm syringe filter. Finally, the mixture was diluted to 50 mL with ultrapure water and subjected to the enrichment and clean-up process, where twenty milligrams of 3D-rGOPFH was added into the prepared sample solution followed by vigorously shaking for 20 min. After magnetically separating and drying, the analytes were desorbed with 1 mL of ethyl acetate for 20 min. The resulting desorption solution was then collected, and 1.0 μL of the solution was injected into the GC-MS/MS for detection.

2.5. Method Validation

A matrix blank was injected in each batch of samples to identify the presence of any cross-contamination and interference during the analysis. To evaluate the applicability of the method, the linearity, LOD (limit of detection), LOQ (limit of quantification), precision, accuracy, and matrix effect were investigated under the optimized extraction conditions. The linearity was estimated using matrix-matched calibration curves by spiking blank samples. The peak areas of each analyte were plotted against their corresponding concentration levels (0.01–100 ng g^{−1}), and then, linear regression analyses were performed on the resulting curves following the minimum least-square method. LOD was determined as the lowest concentration of the spiked analyte with a signal to noise ratio (S/N) of 3 for the target ions. The method LOQ was set at the minimum concentration that could be quantified with acceptable accuracy and precision [33]. For determining the precision of the method, five similar experiments were carried out for blank extracts spiked at 10 ng g^{−1} on the same day and the three consecutive days. To test the accuracy, recovery tests were carried out in real tomato, cucumber, and pakchoi samples at three different levels (5, 25, and 50 ng g^{−1}) with six replicates. The recovery was determined by comparing the calculated amounts of insecticides in the samples with the spiked amounts. The matrix effect was calculated from the calibration curve slope in the matrix and solvent according to the following equation.

$$\text{Matrix effect (\%)} = \left(\frac{\text{Slope of calibration curve in matrix}}{\text{Slope of calibration curve in solvent}} - 1 \right) \times 100$$

2.6. Statistical Analysis

The data were statistically analyzed using statistical software IBM SPSS statistics, version 19. Saphiro–Wilk test was used to check the normality of the results, and Box-Cox transformation was used for variables with non-normal distribution. The homoscedasticity was examined using Levene's test, after which the results were subjected to a one-way analysis of variances (ANOVA). Tukey test was used to reveal the individual differences between groups. Unless noted otherwise, *p* < 0.05 was considered as significant.

3. Results and Discussion

3.1. Investigation of 3D-rGOPFH

3.1.1. Characterization of 3D-rGOPFH

The morphologies of as-prepared PNT and 3D-rGOPFH were observed under the digital camera, SEM, and TEM. In Figure 2a, PNT possessed tubular form with a length of about 5 μm and a diameter of about dozens of nanometers. After being self-assembled with GO and Fe_3O_4 nanoparticles, the well-defined black hydrogel in a cylindrical shape floated on the top of the system. According to figure, only a transparent solution was left at the bottom of the conical flask after the hydrothermal reaction, and no separated Fe_3O_4 nanoparticles and GO sheets could be elsewhere, suggesting that the ternary system, containing PNT, GO and Fe_3O_4 nanoparticles, self-assembled adequately (Figure 2b). The 3D-rGOPFH exhibited an interconnected network architecture with uniformly dispersed pores (Figure 2c,d). The PNT was evenly attached on the surface of rGO sheets (Figure 2e); meanwhile, some of PNT were dispersed between rGO sheets, avoiding the stacking or aggregation of rGO sheets in two-dimension magnetic graphene 2D-G- Fe_3O_4 (Figure 2f).

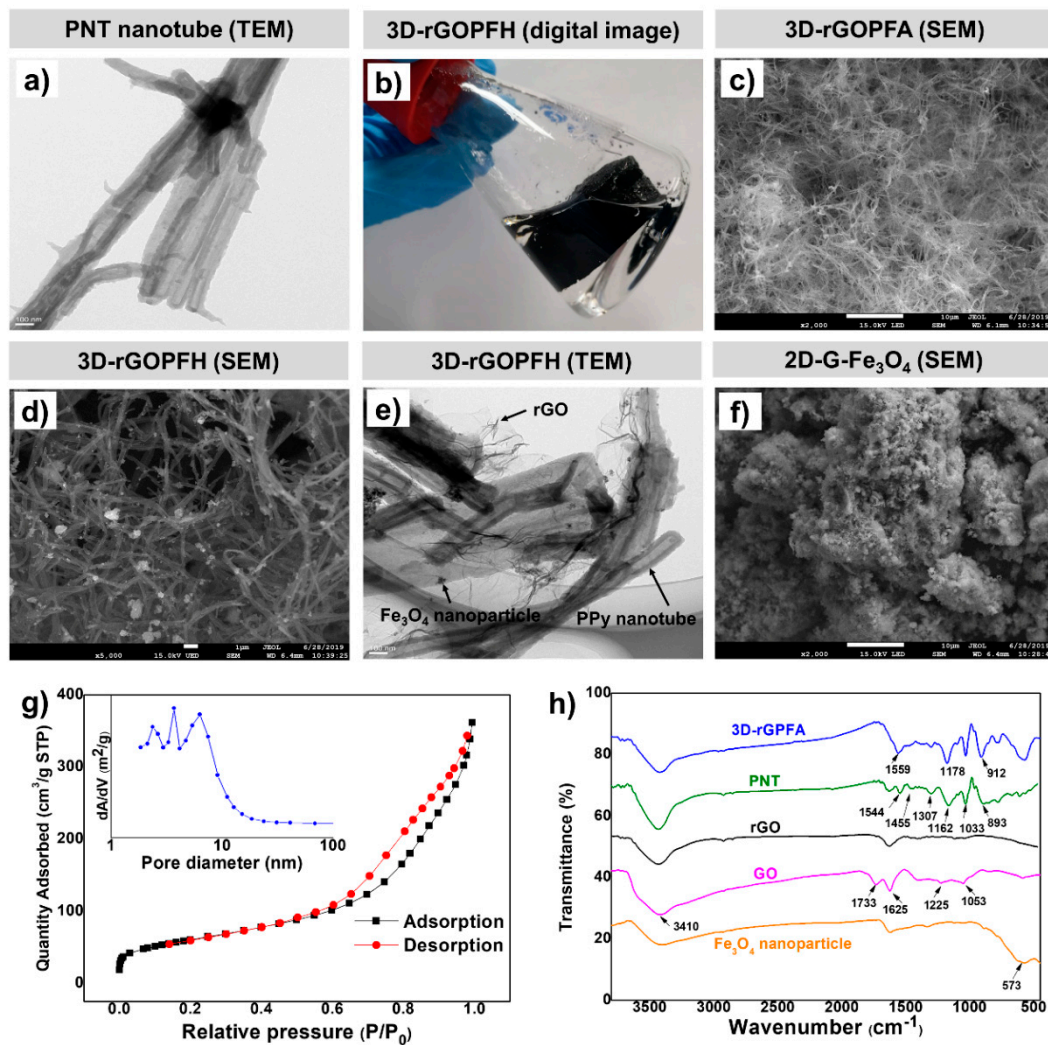


Figure 2. (a–f) The morphologies of the as-prepared materials were observed using SEM, TEM, and digital camera. (g) The nitrogen adsorption-desorption isotherm and pore size distribution analysis of 3D-rGOPFH. (h) FT-IR spectra of GO, rGO, PNT, Fe_3O_4 nanoparticles and 3D-rGOPFH.

The 3D architecture of 3D-rGOPFH was further validated by using the Brunauer–Emmett–Teller (BET) and Barrett–Joyner–Halenda (BJH) techniques, respectively. In Figure 2g, the nitrogen adsorption-desorption isotherm corresponding to 3D-rGOPFH displayed the type II hysteresis loop, characteristic to the pores with different pore sizes. The specific surface area and total pore volume of 3D-rGOPFH were determined to be $237 \text{ m}^2 \text{ g}^{-1}$ and $0.276 \text{ cm}^3 \text{ g}^{-1}$, respectively. The pore size distribution was calculated by density functional theory to be in the range from 1 to 10 nm.

Figure 2h represents the FT-IR spectra of the fabricated GO, rGO, PNT, Fe_3O_4 nanoparticles, and 3D-rGOPFH. The main characteristic peaks of rGO (1625 cm^{-1}), PNT (1544 cm^{-1} and 1455 cm^{-1}), and Fe_3O_4 nanoparticles (574 cm^{-1}) were included in the FT-IR spectra of 3D-rGOPFH, suggesting the successful fabrication of target material. Additionally, the successful fabrication of 3D-rGOPFH was further demonstrated by XRD spectra (Figure S1a).

The magnetic properties of the as-fabricated 3D-rGOPFH at room temperature were measured using a vibrating sample magnetometer. The magnetic hysteresis loops show that 3D-rGOPFH has a super-paramagnetic property with maximum saturation magnetization (M_s) at 40.3 emu g^{-1} (Figure S1b).

3.1.2. Selection of 3D-rGOPFH

To identify the optimal 3D-rGOPFH, eight 3D-rGOPFH with different loading amounts of PNT (20:1, 16:1, 12:1, 8:1, 4:1, 2:1, 1:1 and 1:2) were synthesized and compared. The effect of these sorbents on the extraction efficiency was investigated for the determination of thirteen insecticides. According to Figure S2, higher extraction efficiency was obtained when the ratio of the mass of PNT (m_{PNT}) to that of GO (m_{GO}) was 12:1. The extraction efficiency gradually decreased as the $m_{\text{PNT}}:m_{\text{GO}}$ ratio was changed from 12:1 to 1:2. When more amounts of PNT were introduced, the extraction efficiency was improved, owing to the filling effect and strong adsorption forces of PNT. As the PNT ratio ($>12:1$) was further increased, its adsorption efficiency decreased. An excessive PNT in the 3D-rGOPFH would lead to a greater difficulty in maintaining a fixed gel shape. The results indicated the deterioration of a 3D structure of 3D-rGOPFH might reduce extraction efficiency.

3.1.3. Comparison of the Extraction Efficiency of 3D-rGOPFH with Different Sorbents

For evaluating the extraction ability of the 3D-rGOPFH and elucidating its extraction compatibility for insecticides, four different types of magnetic sorbents, namely Fe_3O_4 , 2D-G- Fe_3O_4 , PNT/ Fe_3O_4 , and 3D-G- Fe_3O_4 , were used and compared to extract thirteen insecticides in the same extraction conditions. Figure 3 shows that all materials possess the ability to extract insecticides, while 3D-rGOPFH performs the best. Compared to Fe_3O_4 , the extraction recoveries were improved by using 2D-G- Fe_3O_4 and PNT/ Fe_3O_4 , suggesting the incorporated rGO sheets or PNT possessed higher BET and provided more interaction forces with analytes [34]. When the structure of 2D-G- Fe_3O_4 was transformed from 2D to 3D, the extraction recoveries were further improved by using 3D-G- Fe_3O_4 . Although the recovery was significantly improved, 3D-G- Fe_3O_4 showed distinct differences in extraction recovery for different types of insecticides. For triazoles, pyrethroids, and OCPs, the recoveries of 70–85% were satisfactory. However, the recoveries corresponding to some OPPs and carbamates were obviously lower (40–70%). In contrast, the recoveries of 3D-rGOPFH for all thirteen insecticides were between 65–90%. Compared to 3D-G- Fe_3O_4 , the improvement ratios of recovery for 3D-rGOPFH were 21–73% for four OPPs (quinalphos, phorate, chlorpyrifos, and phosalone) and two carbamates (pirimor and carbaryl) insecticides, which were distinctly higher than that (8–24%) for two triazoles (myclobutanil and diniconazole), two pyrethroids (bifenthrin and lambda-cyhalothrin), and one OCPs (2,4'-DDT). One-way ANOVA analysis was performed to test the significance between 3D-rGOPFH and 3D-G- Fe_3O_4 . For all insecticides, except isocarbophos and mirex, the extraction recovery was statistically significant ($p < 0.05$). Triazoles, pyrethroids, and OCPs mainly contained aromatic ring group; π - π stacking interaction and hydrophobic force were the main interaction forces between sorbents and analytes in the extraction process [32]. In contrast, most of the OPPs and carbamates insecticides contained more polar (phosphate and amine) groups, and multiple interaction forces may

be involved between sorbents and analytes, such as hydrogen bonding, electrostatic force, and π - π stacking interaction. After introducing PNT into graphene, new driving forces emerged from hydrogen bonding and electrostatic interaction, and thus the changed surface property/polarity of magnetic graphene assisted the adsorption process. Because of the 3D architecture and multiple adsorption forces, 3D-rGOPFH exhibited adequate superiority in extraction efficiency and compatibility for different types of insecticides.

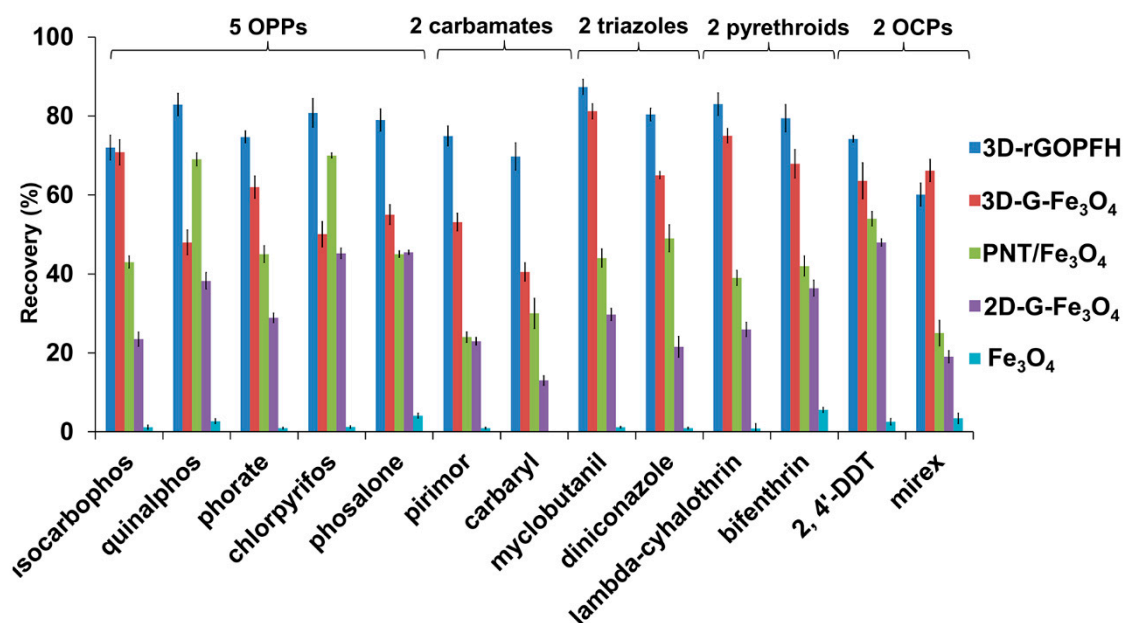


Figure 3. Evaluation of the extraction efficiency for different insecticides using different magnetic sorbents. The standard deviation (SD) bars were marked ($n = 5$).

3.2. Optimization of Extraction Conditions

To achieve a higher recovery for the target insecticides, different experimental conditions were optimized. Each parameter was optimized while all the others were fixed at their optimized value. Ultrapure water or methanol-water solvent with spiked insecticide concentration at 50 ng g^{-1} was used to examine the extraction recovery. All the experiments were carried out in triplicate, and the means of results were reported.

Desorption of the analytes from the magnetic sorbent was investigated using the commonly used organic solvent, i.e., ethyl acetate, acetone/chloroform ($v/v = 1:1$), acetone, acetone/ethyl acetate ($v/v = 1:1$), and acetonitrile. Among the potential eluent solvents, ethyl acetate as an aprotic solvent with intermediate polarity exhibited the highest eluting power for all insecticides, showing significant difference from the protic solvent acetonitrile (Figure S3a). Thus, ethyl acetate was selected as the desorption solvent. For completely desorbing the analytes from the 3D-rGOPFH, the influence of the desorption time from 2 to 40 min was also studied. The best desorption efficiency was achieved when 20 min was used (Figure S3b).

To assure the maximum adsorption amount of analyte, the effect of extraction time on the extraction efficiency was optimized by increasing the time from 2 to 40 min. As shown in Figure S3c, for most of the insecticides, 20 min was needed to achieve the optimal adsorption amount. For mirex and bifenthrin, 2 min was enough to get equilibrium, nevertheless, extraction recovery decreased slightly when a longer time was used. The reduction in extraction efficiency may be attributed to back-extraction effect after the equilibrium due to the issue of solubility of these analytes in water [35]. To achieve an appropriate extraction efficiency for all the insecticides, 20 min was selected for subsequent experiments. Meanwhile, the effect of the amount of the 3D-rGOPFH on the extraction was studied by using different amounts ranging from 2.5 to 30 mg. As shown in Figure S3d, the maximum extraction efficiency was obtained at

20 mg of 3D-rGOPFH. No further increase in the sample recovery rate can be observed when a larger absorbent dose was applied. In subsequent experiments, effects of the sample solution pH (from 3 to 11) and ionic strength (with NaCl addition from 0 to 15% (*m/v*)) on the extraction efficiency were explored. The results indicated that there was no need to adjust the pH of the sample solution (Figure S3e) during the extraction process, and the addition of NaCl was not necessary (Figure S3f).

Because methanol was adopted in the real-world sample analysis, the effect of methanol content on the MSPE of insecticides should be discussed. The addition of methanol was investigated over the range of 0–50% (*v/v*). In Figure S3g, the results demonstrated that the use of a small amount of methanol (0–20%) did not affect the extraction efficiency.

To examine whether the target analytes were desorbed sufficiently, the effect of the volume of ethyl acetate from 0.5 to 2.0 mL was further explored. Figure S3h clearly shows that 1 mL is the optimal desorption volume. No further increase in the sample recovery rate was noticed when a larger desorption volume was applied. Single time desorption was sufficient for achieving high recovery.

3.3. Analytical Performance

In Table 1, the matrix-matched standard curves for all insecticides exhibited good linearities in the range of 0.1–100 ng g⁻¹. The determination coefficients (*R*²) were satisfactory, with the values from 0.9975 to 0.9998. The LOD values of all insecticides ranged from 0.006 to 0.03 ng g⁻¹, depending upon the type of the analyte, while the LOQ values were 5 ng g⁻¹ for thirteen insecticides analyzed, and these values were sufficient to achieve the required sensitivity for target insecticides analyses. Additionally, the intra-day relative standard deviations (RSDs) and inter-day RSDs were in the range of 2.8–7.1% and 3.5–8.8%, respectively. The validation results indicated good linearity, sensitivity, and precision of the method.

Table 1. The linearity, determination coefficients, LOD, LOQ, and RSD for insecticides in the tomato sample.

Analyte	Regression Curves	Linearity (ng g ⁻¹)	<i>R</i> ²	LODs (ng g ⁻¹)	LOQs (ng g ⁻¹)	MRLs (ng g ⁻¹)	RSD	
							Intraday (<i>n</i> = 5)	Inter-Day (<i>n</i> = 15)
Isocarbophos	Y = 17,453X + 4380	5–100	0.9993	0.03	5	50	4.5	5.1
Quinalphos	Y = 162,933X – 43,204	5–100	0.9998	0.009	5	-	3.6	4.5
Phorate	Y = 23,107X + 9314	5–100	0.9975	0.009	5	10	4.6	7.0
Chlorpyrifos	Y = 91,978X – 27,323	5–100	0.9986	0.009	5	10–1000	2.5	4.5
Phosalone	Y = 202,703X + 34,570	5–100	0.9995	0.01	5	1000	6.8	8.8
Pirimor	Y = 42,473X + 37,167	5–100	0.9996	0.01	5	10–5000	3.3	5.2
Carbaryl	Y = 39,737X + 39,214	5–100	0.9990	0.01	5	20–5000	2.8	6.4
Myclobutanil	Y = 637,361X – 4792	5–100	0.9972	0.006	5	50–3000	3.4	3.7
Diniconazole	Y = 162,443X – 37,706	5–100	0.9991	0.006	5	50	5.5	5.2
Lambda-cyhalothrin	Y = 111,654X – 53,779	5–100	0.9992	0.03	5	10–5000	7.1	3.6
Bifenthrin	Y = 698,826X – 193,428	5–100	0.9993	0.01	5	50–4000	2.6	3.5
2, 4'-DDT	Y = 121,476X – 22,140	5–100	0.9992	0.01	5	50–200	4.8	4.1
Mirex	Y = 239,134X – 137,874	5–100	0.9998	0.01	5	10	3.0	4.2

MRLs represent the maximum residue limits of insecticides in vegetables, as recommended by the National Food Safety Standard (China, GB 2763-2019). Intraday data and inter-day data were evaluated using one-way ANOVA with “day” as the grouping variable.

To further evaluate the applicability of the developed method, it was used for the determining of the insecticide residues in tomato, cucumber, and pakchoi samples, bought from the local supermarket. According to Table 2, 4.7 ng g⁻¹ bifenthrin and 4.9 ng g⁻¹ lambda-cyhalothrin were detected in cucumber and pakchoi, respectively, which were lower than the MRLs. The recovery of thirteen insecticides (79.2–109.4%) were in the range of 70–120%, as set by the European Commission, Health and Consumer Protection Directorate-General [33]. The RSDs were below 11.2%, meeting the requirements of pesticide residue analysis (RSD ≤ 20%) [33].

Table 2. Determinations of the insecticides and recovery in tomato, cucumber, and pakchoi samples.

Analytes	Spiked (ng g ⁻¹)	Tomato			Cucumber			Pakchoi		
		Found (ng g ⁻¹)	Recovery (%)	RSD (%)	Found (ng g ⁻¹)	Recovery (%)	RSD (%)	Found (ng g ⁻¹)	Recovery (%)	RSD (%)
Isocarbophos	0	ND			ND			ND		
	5	5.3 ± 0.3	105.3	6.5	4.8 ± 0.2	96.4	5.0	5.2 ± 0.3	104.3	5.8
	25	24.6 ± 0.9	98.5	3.8	23.7 ± 1.1	94.6	4.5	26.5 ± 1.0	106.1	3.7
	50	50.8 ± 2.6	101.6	5.1	51.7 ± 1.9	103.4	3.9	46.7 ± 2.8	93.3	5.9
Quinalphos	0	ND			ND			ND		
	5	4.4 ± 0.2	87.7	3.6	4.8 ± 0.3	95.7	5.6	5.2 ± 0.2	104.2	4.5
	25	23.7 ± 1.1	94.6	4.8	22.6 ± 1.4	90.2	6.3	25.7 ± 1.0	103.0	3.7
	50	49.2 ± 2.3	98.3	4.7	48.3 ± 2.3	96.5	4.7	46.3 ± 3.1	92.6	6.7
Phorate	0	ND			ND			ND		
	5	4.9 ± 0.6	97.1	11.2	4.0 ± 0.4	79.2	9.8	4.9 ± 0.4	82.3	8.0
	25	24.4 ± 1.8	97.7	7.2	24.6 ± 1.6	98.3	6.4	26.8 ± 1.6	107.0	5.8
	50	50.7 ± 2.0	101.4	4.0	47.3 ± 1.6	94.5	3.4	46.2 ± 1.5	92.4	3.2
Chlorpyrifos	0	ND			ND			ND		
	5	5.1 ± 0.2	101.9	4.2	5.3 ± 0.4	105.6	6.8	5.2 ± 0.2	104.3	4.5
	25	24.1 ± 0.9	96.4	3.8	25.6 ± 1.7	102.5	6.7	24.1 ± 0.9	96.5	3.7
	50	48.3 ± 1.3	96.5	2.7	46.8 ± 2.6	93.6	5.5	47.9 ± 1.9	95.8	3.9
Phosalone	0	ND			ND			ND		
	5	4.9 ± 0.4	97.2	8.5	5.1 ± 0.2	102.8	3.6	4.8 ± 0.2	96.7	4.1
	25	23.8 ± 0.9	95.1	3.6	23.6 ± 0.6	94.6	2.5	22.6 ± 0.9	90.3	3.8
	50	47.3 ± 2.5	94.6	5.4	48.3 ± 1.2	96.6	2.4	46.4 ± 1.3	92.9	2.7
Pirimor	0	ND			ND			ND		
	5	5.5 ± 0.3	109.4	4.8	5.0 ± 0.3	100.5	6.2	5.2 ± 0.1	104.5	2.8
	25	25.3 ± 1.4	101.3	5.6	24.6 ± 1.0	98.4	4.1	24.7 ± 0.9	98.6	3.7
	50	47.6 ± 1.6	95.2	3.3	52.4 ± 1.6	104.7	3.0	50.1 ± 2.6	100.2	5.1
Carbaryl	0	ND			ND			ND		
	5	5.4 ± 0.5	107.7	9.8	5.4 ± 0.2	108.7	4.2	4.7 ± 0.3	94.5	6.4
	25	24.3 ± 2.6	97.2	10.9	24.6 ± 1.2	98.4	4.8	23.5 ± 1.3	94.0	5.5
	50	48.7 ± 2.8	97.4	5.7	52.8 ± 3.6	105.6	6.8	49.4 ± 3.7	98.7	7.6
Myclobutanil	0	ND			ND			ND		
	5	4.8 ± 0.3	95.3	6.5	5.0 ± 0.2	100.5	3.2	5.0 ± 0.3	100.7	5.3
	25	24.2 ± 1.3	96.9	5.4	24.8 ± 0.8	99.2	5.3	24.7 ± 1.9	98.7	7.7
	50	50.6 ± 1.6	101.1	3.1	49.6 ± 1.4	99.1	2.8	49.3 ± 1.2	98.5	2.5
Diniconazole	0	ND			ND			ND		
	5	5.2 ± 0.2	103.1	3.5	4.3 ± 0.2	85.2	5.1	5.2 ± 0.3	104.9	6.5
	25	23.9 ± 0.7	95.5	2.8	24.3 ± 0.5	97.3	1.9	23.9 ± 1.8	95.4	7.6
	50	51.9 ± 3.6	103.8	6.9	48.7 ± 3.0	97.3	6.2	52.7 ± 0.9	105.3	1.7
Lambda-cyhalothrin	0	ND			ND			ND		
	5	4.4 ± 0.2	88.8	3.8	5.0 ± 0.2	99.0	3.6	10.4 ± 0.4	109.0	4.3
	25	26.5 ± 1.7	105.9	6.4	26.2 ± 0.7	104.8	2.8	29.5 ± 0.7	98.4	2.5
	50	47.6 ± 1.8	95.1	3.7	53.9 ± 2.4	107.8	4.5	53.9 ± 1.8	98.0	3.4
Bifenthrin	0	ND			ND			ND		
	5	5.1 ± 0.3	102.5	5.8	9.6 ± 0.6	98.0	5.8	5.3 ± 0.2	106.2	4.5
	25	25.5 ± 1.5	101.8	5.9	30.8 ± 0.8	104.4	2.6	24.2 ± 1.2	96.8	5.1
	50	49.8 ± 2.1	99.7	4.2	53.6 ± 2.0	97.8	3.8	48.6 ± 1.3	97.2	2.6
2, 4'-DDT	0	ND			ND			ND		
	5	4.7 ± 0.3	93.5	7.3	5.1 ± 0.2	102.6	3.8	5.2 ± 0.4	104.7	8.3
	25	22.5 ± 1.1	90.1	5.1	26.8 ± 1.6	107.2	5.8	24.7 ± 0.9	98.7	3.5
	50	45.6 ± 1.8	91.2	4.0	46.2 ± 3.7	92.4	8.0	53.3 ± 2.6	106.7	4.8
Mirex	0	ND			ND			ND		
	5	4.4 ± 0.4	87.3	8.1	4.8 ± 0.3	95.3	7.2	4.9 ± 0.2	98.4	4.3
	25	23.5 ± 1.5	94.0	6.4	22.9 ± 1.3	91.4	5.5	26.4 ± 1.4	105.6	5.2
	50	51.9 ± 2.9	103.7	5.6	52.7 ± 2.7	105.4	5.1	52.4 ± 1.7	104.7	3.2

Found (mean ± SD, $n = 6$), ND indicates that the concentration level of the sample is less than LOQ.

Generally, the co-elution of matrix constituents can interfere with the ionization of the target compounds, causing ion enhancement or suppression. The matrix effect caused a signal enhancement or suppression of the analytes, which could affect the quality of the quantitative data, achieved from the method. The matrix effect values were in the range of -56.4 to 40.5% for these three vegetable extracts without any treatment, and the effect was serious and could not be ignored for most of the insecticides. After the extraction with 3D-rGOPFH, the matrix effect values were reduced to neglectable levels for all of the insecticides, and the values were from -9.1% to 16.4% (Table S2). Furthermore, very clean spectra with a low baseline were obtained in the total ion chromatograms of spiked or un-spiked blank vegetables (Figure 4). These results demonstrated that 3D-rGOPFH could be an efficient MSPE extraction sorbent for reducing the matrix interferences.

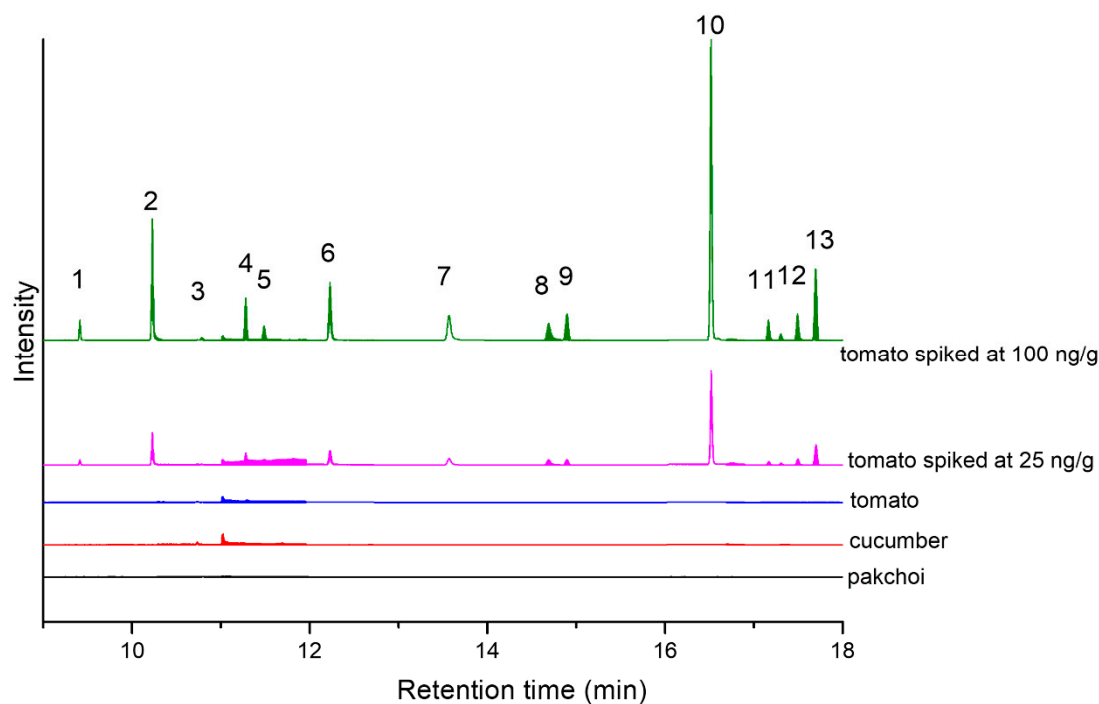


Figure 4. MSPE-GC-MS/MS chromatograms for spiked/un-spiked blank vegetables. The chromatogram peaks marked 1 to 13 represent isocarbophos, quinalphos, phorate, chlorpyrifos, phosalone, pirimor, carbaryl, myclobutanil, diniconazole, lambda-cyhalothrin, bifenthrin, 2,4'-DDT, and mirex, respectively.

3.4. The Reusability and Batch Difference of 3D-rGOPFH

The reusability of the sorbent in the MSPE procedure can reduce the cost of analysis. To investigate the mechanical stability and reusability of the 3D-rGOPFH, the recovered 3D-rGOPFH sorbent was rinsed with 2 mL of acetone for three times. After such washing, no sample residue was detected with GC-MS/MS, and the sorbent was reused for the next extraction cycle. The 3D-rGOPFH sorbent was used at least ten times without a significant loss of the adsorption ability, which demonstrated that the fabricated 3D-rGOPFH via hydrothermal reduction possessed high stability. The robustness for the preparation of different batches of the 3D-rGOPFH has also been examined. The adsorption ability of the 3D-rGOPFH, synthesized in five batches, exhibits no obvious changes with the RSDs below 8.7% from batch to batch.

3.5. Comparison with Other Methods

To comprehensively estimate the developed method, it was compared to several other reported methods, which determined insecticides in vegetables (Table 3). Although the different sorbent materials were utilized in these works in similar matrices for insecticides, these sorbents generally demonstrated lower selectivity to only a few analytes. In comparison, 3D-rGOPFH was able to adsorb different classes of insecticides from the sample and provided satisfactory extraction efficiency with recoveries higher than 79.2%. Unlike other reported methods, no matrix effect was observed in our developed sample preparation method. Also, the MSPE operations of this work were simpler than those reported in the literature. No repeated desorption process, nitrogen blowing, and redissolution were employed, simplifying sample preparation. These results demonstrate that the current method is adequate for the pretreatment of the multiresidue insecticides in vegetable samples. Despite its obvious superiorities, the limitation of this method is that the sample extraction and separation/detection are carried out off-line as well as a drying process is required to remove moistures after magnetic separation of the sorbent. Moreover, the preparation process of 3D-rGOPFH nanohybrid is slightly

time-consuming. We will focus on these issues in future research to improve the efficiency of the current method for determining various pesticide residues in various samples.

Table 3. Comparison of the current study with other MSPE techniques used for vegetable sample preparation.

Method	Analyte	Linearity (ng g ⁻¹)	LOD (ng g ⁻¹)	Recovery (%)	Matrix Effect	Nitrogen Blowing and Reconstitution	Desorption Times	Refs
MSPE-GC- μ ECD	3 insecticides	1–20	0.23–0.3	82–113	not reported	yes	1	[36]
MSPE-GC- μ ECD	3 insecticides	0.1–5	0.07–0.13	72.8–109.6	not reported	yes	1	[37]
MMIP-HPLC-UV	1 acephate	10–5000	0.1	89.2–93.4	not reported	yes	3	[38]
MSPE-HPLC-UV	6 pyrethroids	5–500	0.63–1.2	76–99.5	not reported	yes	1	[39]
MSPE-HPLC-DAD	6 carbamates	5–200	0.58–2.06	90.34–101.98	not reported	yes	3	[40]
MSPE-GC-MS/MS	5 OPPs, 2 OCPs, 2 carbamates, 2 pyrethroids, and 2 triazoles	0.1–100	0.006–0.03	79.2–109.4	no	no	1	This work

μ ECD: micro electron capture detector; MMIP: magnetic molecularly imprinted polymers; HPLC: high-performance liquid chromatography; UV: ultraviolet detector; DAD: diode array detector.

4. Conclusions

In this study, a 3D-rGOPFH nanohybrid was successfully fabricated by a self-assembly of rGO nanosheets decorated with PNT and Fe₃O₄ nanoparticles. Then the nanohybrid was used as MSPE sorbent for simultaneous preconcentration of thirteen insecticides in vegetable samples followed by GC-MS/MS determination. PNT that functions as a spacer avoids the stacking or aggregation of graphene sheets and improves the affinity of material for analytes via providing multiple adsorption interactions, such as hydrogen bonding, electrostatic interaction, π - π stacking interaction, and hydrophobic interaction force. Compared to other reported Fe₃O₄, 2D-G-Fe₃O₄, PNT/Fe₃O₄, and 3D-G-Fe₃O₄ sorbents, 3D-rGOPFH exhibits better adsorption efficiency and analyte-compatibility for different classes of insecticides. Furthermore, 3D-rGOPFH effectively excludes the interfering compounds, and clean analytes were obtained by elution and analyzed using GC-MS/MS. The magnetic nanohybrids help convenient separation of sorbent from the sample solution by an external magnetic field without the need for centrifugation or filtration procedures. In all cases, a low limit of detections of 0.006–0.03 ng g⁻¹ and satisfactory recoveries of 79.2–109.4% were obtained with RSD \leq 8.8%. These results indicated the developed method is a facile, environment-friendly, time and energy-saving, and sensitive sample preparation technique to determine multi-insecticide residues. The proposed method is expected to be widely applied for determining other organic pollutants in different samples in our further study.

Supplementary Materials: The following are available online at <http://www.mdpi.com/2076-3417/10/16/5665/s1>, Figure S1: (a) XRD analysis of GO, rGO, PNT, Fe₃O₄ nanoparticle, and 3D-rGOPFH. (b) VSM magnetization curve of 3D-rGOPFH., Figure S2: Effect of different loading amounts of PNT ($m_{\text{PNT}}:m_{\text{GO}} = 20:1, 16:1, 12:1, 8:1, 4:1, 2:1, 1:1, \text{ and } 1:2$) on extraction efficiency., Figure S3: Effect of (a) desorption solvent, (b) desorption time, (c) extraction time, (d) sorbent dosage, (e) pH, (f) ionic strength, (g) methanol content, and (h) desorption volume on extraction efficiency of MSPE by using 3D-rGOPFH. Table S1: Chemical structure, type, molecular weights, retention time, ion transition and Log *p* of the target compounds, Table S2: Matrix effect values of insecticides in tomato, cucumber, and pakchoi samples.

Author Contributions: Conceptualization, S.W. and H.L.; methodology, S.W.; software, S.W.; validation, S.W. and S.L.; investigation, S.W.; writing—original draft preparation, S.W., X.L. (Xiuqin Li), M.L., X.L. (Xianjiang Li), X.L. (Xiaomin Li), Q.Z., and H.L.; writing—review and editing, S.W. and H.L.; supervision, H.L.; funding acquisition, S.W. and H.L. All authors have read and agreed to the published version of the manuscript.

Funding: This research was funded by the National Key R&D Program of China (2019YFC1604800).

Conflicts of Interest: The authors declare no conflict of interest. The funders had no role in the design of the study; in the collection, analyses, or interpretation of data; in the writing of the manuscript, or in the decision to publish the results.

References

1. Fenner, K.; Canonica, S.; Wackett, L.P.; Elsner, M. Evaluating pesticide degradation in the environment: Blind spots and emerging opportunities. *Science* **2013**, *341*, 752. [[CrossRef](#)] [[PubMed](#)]
2. Masia, A.; Suarez-Varela, M.M.; Llopis-Gonzalez, A.; Pico, Y. Determination of pesticides and veterinary drug residues in food by liquid chromatography-mass spectrometry: A review. *Anal. Chim. Acta* **2016**, *936*, 40–61. [[CrossRef](#)] [[PubMed](#)]
3. Dell'Oro, D.; Casamassima, F.; Gesualdo, G.; Iammarino, M.; Mambelli, P.; Nardelli, V. Determination of pyrethroids in chicken egg samples: Development and validation of a confirmatory analytical method by gas chromatography/mass spectrometry. *Int. J. Food Sci. Technol.* **2014**, *49*, 1391–1400. [[CrossRef](#)]
4. Nedaei, M.; Salehpour, A.R.; Mozaffari, S.; Yousefi, S.M.; Yousefi, S.R. Determination of organophosphorus pesticides by gas chromatography with mass spectrometry using a large-volume injection technique after magnetic extraction. *J. Sep. Sci.* **2014**, *37*, 2372–2379. [[CrossRef](#)] [[PubMed](#)]
5. Jia, C.; Zhu, X.; Wang, J.; Zhao, E.; He, M.; Chen, L.; Yu, P. Combination of dispersive solid-phase extraction and salting-out homogeneous liquid-liquid extraction for the determination of organophosphorus pesticides in cereal grains. *J. Sep. Sci.* **2014**, *37*, 1862–1866. [[CrossRef](#)] [[PubMed](#)]
6. Li, X.; Li, H.; Ma, W.; Guo, Z.; Li, X.; Song, S.; Tang, H.; Li, X.; Zhang, Q. Development of precise GC-EI-MS method to determine the residual fipronil and its metabolites in chicken egg. *Food Chem.* **2019**, *281*, 85–90. [[CrossRef](#)]
7. Li, J.-W.; Wang, Y.-L.; Yan, S.; Li, X.-J.; Pan, S.-Y. Molecularly imprinted calixarene fiber for solid-phase microextraction of four organophosphorus pesticides in fruits. *Food Chem.* **2016**, *192*, 260–267. [[CrossRef](#)]
8. Cacho, J.; Campillo, N.; Viñas, P.; Hernández-Córdoba, M. In situ ionic liquid dispersive liquid-liquid microextraction coupled to gas chromatography-mass spectrometry for the determination of organophosphorus pesticides. *J. Chromatogr. A* **2018**, *1559*, 95–101. [[CrossRef](#)]
9. Wang, C.; Wu, Q.; Wu, C.; Wang, Z. Application of dispersion-solidification liquid-liquid microextraction for the determination of triazole fungicides in environmental water samples by high-performance liquid chromatography. *J. Hazard. Mater.* **2011**, *185*, 71–76. [[CrossRef](#)]
10. Hou, X.; Tang, S.; Wang, J. Recent advances and applications of graphene-based extraction materials in food safety. *TrAC Trends Anal. Chem.* **2019**, *119*, 115603. [[CrossRef](#)]
11. Wang, S.; Xiao, C.; Guo, L.; Ling, L.; Li, M.; Li, H.; Guo, X. Rapidly quantitative analysis of γ -glutamyltranspeptidase activity in the lysate and blood via a rational design of the molecular probe by matrix-assisted laser desorption ionization mass spectrometry. *Talanta* **2019**, *205*, 120141. [[CrossRef](#)] [[PubMed](#)]
12. Wang, L.; Zang, X.; Chang, Q.; Wang, C.; Wang, Z. A graphene-coated magnetic nanocomposite for the enrichment of fourteen pesticides in tomato and rape samples prior to their determination by gas chromatography-mass spectrometry. *Anal. Methods* **2014**, *6*, 253–260. [[CrossRef](#)]
13. Wang, W.; Ma, X.; Wu, Q.; Wang, C.; Zang, X.; Wang, Z. The use of graphene-based magnetic nanoparticles as adsorbent for the extraction of triazole fungicides from environmental water. *J. Sep. Sci.* **2012**, *35*, 2266–2272. [[CrossRef](#)] [[PubMed](#)]
14. Qiu, B.; Xing, M.; Zhang, J. Recent advances in three-dimensional graphene based materials for catalysis applications. *Chem. Soc. Rev.* **2018**, *47*, 2165–2216. [[CrossRef](#)]
15. Sitko, R.; Zawisza, B.; Malicka, E. Graphene as a new sorbent in analytical chemistry. *TrAC Trends Anal. Chem.* **2013**, *51*, 33–43. [[CrossRef](#)]
16. Li, N.; Chen, J.; Shi, Y.P. Magnetic polyethyleneimine functionalized reduced graphene oxide as a novel magnetic solid-phase extraction adsorbent for the determination of polar acidic herbicides in rice. *Anal. Chim. Acta* **2017**, *949*, 23–34. [[CrossRef](#)]
17. Ma, G.; Zhang, M.; Zhu, L.; Chen, H.; Liu, X.; Lu, C. Facile synthesis of amine-functional reduced graphene oxides as modified quick, easy, cheap, effective, rugged and safe adsorbent for multi-pesticide residues analysis of tea. *J. Chromatogr. A* **2018**, *1531*, 22–31. [[CrossRef](#)]
18. Wu, Z.S.; Yang, S.; Sun, Y.; Parvez, K.; Feng, X.; Mullen, K. 3D nitrogen-doped graphene aerogel-supported Fe₃O₄ nanoparticles as efficient electrocatalysts for the oxygen reduction reaction. *J. Am. Chem. Soc.* **2012**, *134*, 9082–9085. [[CrossRef](#)]

19. Mahpishanian, S.; Sereshti, H. Three-dimensional graphene aerogel-supported iron oxide nanoparticles as an efficient adsorbent for magnetic solid phase extraction of organophosphorus pesticide residues in fruit juices followed by gas chromatographic determination. *J. Chromatogr. A* **2016**, *1443*, 43–53. [[CrossRef](#)]
20. Tang, B.; Wang, S.; Zhang, J.; Wang, Z.; He, Y.; Huang, W. Three-dimensional graphene monolith-based composite: Superiority in properties and applications. *Int. Mater. Rev.* **2017**, *63*, 204–225. [[CrossRef](#)]
21. Jamróz, E.; Kopel, P.; Tkaczewska, J.; Dordevic, D.; Jancikova, S.; Kulawik, P.; Milosavljevic, V.; Dolezelikova, K.; Smerkova, K.; Svec, P. Nanocomposite Furcellaran Films—The Influence of Nanofillers on Functional Properties of Furcellaran Films and Effect on Linseed Oil Preservation. *Polymers* **2019**, *11*, 2046. [[CrossRef](#)] [[PubMed](#)]
22. Zhang, C.; Chen, Y.; Li, H.; Tian, R.; Liu, H. Facile Fabrication of Three-Dimensional Lightweight RGO/PPy Nanotube/Fe₃O₄ Aerogel with Excellent Electromagnetic Wave Absorption Properties. *ACS Omega* **2018**, *3*, 5735–5743. [[CrossRef](#)] [[PubMed](#)]
23. Silva, B.J.; Lancas, F.M.; Queiroz, M.E. Determination of fluoxetine and norfluoxetine enantiomers in human plasma by polypyrrole-coated capillary in-tube solid-phase microextraction coupled with liquid chromatography-fluorescence detection. *J. Chromatogr. A* **2009**, *1216*, 8590–8597. [[CrossRef](#)] [[PubMed](#)]
24. Hasan, Z.; Jhung, S.H. Removal of hazardous organics from water using metal-organic frameworks (MOFs): Plausible mechanisms for selective adsorptions. *J. Hazard. Mater.* **2015**, *283*, 329–339. [[CrossRef](#)] [[PubMed](#)]
25. Wang, J.; Duan, H.L.; Ma, S.Y.; Zhang, J.; Zhang, Z.Q. Solidification of a Switchable Solvent-Based QuEChERS Method for Detection of 16 Pesticides in Some Fruits and Vegetables. *J. Agric. Food. Chem.* **2019**, *67*, 8045–8052. [[CrossRef](#)]
26. Kittirattanapiboon, K.; Krisnangkura, K. Separation of acylglycerols, FAME and FFA in biodiesel by size exclusion chromatography. *Eur. J. Lipid Sci. Technol.* **2008**, *110*, 422–427. [[CrossRef](#)]
27. Mao, X.; Yan, A.; Wan, Y.; Luo, D.; Yang, H. Dispersive solid-phase extraction using microporous sorbent UiO-66 coupled to gas chromatography-tandem mass spectrometry: A QuEChERS-type method for the determination of organophosphorus pesticide residues in edible vegetable oils without matrix interference. *J. Agric. Food. Chem.* **2019**, *67*, 1760–1770.
28. Wu, J.Y.; Zhang, H.X.; Peng, X.T. Rapid determination of organophosphorus pesticides in edible vegetable oils by direct microextraction using magnetic mesoporous silica microspheres. *Sep. Sci. Plus* **2020**, *3*, 158–166. [[CrossRef](#)]
29. Ying, S.; Zheng, W.; Li, B.; She, X.; Huang, H.; Li, L.; Huang, Z.; Huang, Y.; Liu, Z.; Yu, X. Facile fabrication of elastic conducting polypyrrole nanotube aerogels. *Synth. Met.* **2016**, *218*, 50–55. [[CrossRef](#)]
30. Yang, Y.; Zhao, Y.; Sun, S.; Zhang, X.; Duan, L.; Ge, X.; Lü, W. Self-assembled three-dimensional graphene/Fe₃O₄ hydrogel for efficient pollutant adsorption and electromagnetic wave absorption. *Mater. Res. Bull.* **2016**, *73*, 401–408. [[CrossRef](#)]
31. Cong, H.; Ren, X.; Wang, P.; Yu, S. Macroscopic Multifunctional Graphene-Based Hydrogels and Aerogels by a Metal Ion Induced Self-Assembly Process. *ACS Nano* **2012**, *6*, 2693–2703. [[CrossRef](#)] [[PubMed](#)]
32. Wu, Q.; Zhao, G.; Feng, C.; Wang, C.; Wang, Z. Preparation of a graphene-based magnetic nanocomposite for the extraction of carbamate pesticides from environmental water samples. *J. Chromatogr. A* **2011**, *1218*, 7936–7942. [[CrossRef](#)]
33. European Commission. *Guidance Document on Analytical Quality Control and Method Validation Procedures for Pesticides Residues Analysis in Food and Feed, Supersedes SANTE/11945/2017*; European Commission: Brussels, Belgium, 2015.
34. Han, Q.; Wang, Z.; Xia, J.; Chen, S.; Zhang, X.; Ding, M. Facile and tunable fabrication of Fe₃O₄/graphene oxide nanocomposites and their application in the magnetic solid-phase extraction of polycyclic aromatic hydrocarbons from environmental water samples. *Talanta* **2012**, *101*, 388–395. [[CrossRef](#)] [[PubMed](#)]
35. Hii, T.M.; Basheer, C.; Lee, H.K. Commercial polymeric fiber as sorbent for solid-phase microextraction combined with high-performance liquid chromatography for the determination of polycyclic aromatic hydrocarbons in water. *J. Chromatogr. A* **2009**, *1216*, 7520–7526. [[CrossRef](#)] [[PubMed](#)]
36. Nodeh, H.R.; Sereshti, H.; Gaikani, H.; Kamboh, M.A.; Afsharsaveh, Z. Magnetic graphene coated inorganic-organic hybrid nanocomposite for enhanced preconcentration of selected pesticides in tomato and grape. *J. Chromatogr. A* **2017**, *1509*, 26–34. [[CrossRef](#)] [[PubMed](#)]

37. Sereshti, H.; Afsharsaveh, Z.; Gaikani, H.; Nodeh, H.R. Electroless-coated magnetic three-dimensional graphene with silver nanoparticles used for the determination of pesticides in fruit samples. *J. Sep. Sci.* **2018**, *41*, 1567–1575. [[CrossRef](#)]
38. Gao, L.; Piao, C.; Chen, L. Determination of Acephate in Vegetables by Magnetic Molecularly Imprinted Polymer Isolation Coupled with High-Performance Liquid Chromatography. *Anal. Lett.* **2014**, *48*, 752–765. [[CrossRef](#)]
39. Jiang, C.; Sun, Y.; Yu, X.; Gao, Y.; Zhang, L.; Wang, Y.; Zhang, H.; Song, D. Liquid-solid extraction coupled with magnetic solid-phase extraction for determination of pyrethroid residues in vegetable samples by ultra fast liquid chromatography. *Talanta* **2013**, *114*, 167–175. [[CrossRef](#)]
40. Li, N.; Chen, J.; Shi, Y.P. Magnetic graphene solid-phase extraction for the determination of carbamate pesticides in tomatoes coupled with high performance liquid chromatography. *Talanta* **2015**, *141*, 212–219. [[CrossRef](#)]



© 2020 by the authors. Licensee MDPI, Basel, Switzerland. This article is an open access article distributed under the terms and conditions of the Creative Commons Attribution (CC BY) license (<http://creativecommons.org/licenses/by/4.0/>).